論文

스월 인젝터의 동특성에 대한 수치해석 연구

박홍복*

Dynamic Characteristics Simulation for a Simplex Swirl Injector

Hongbok Park*

ABSTRACT

A fully nonlinear model accounting for swirling effect has been applied in analyzing the dynamic response for a classical swirl injector. The current work applied highly accurate Boundary Element Methods (BEMs) in assessing its static and dynamic characteristics. On the basis of moving surface treatment method and surface instability study, which are obtained from the previous static characteristics analysis in pressure-swirl injectors, this work was expanded for analyzing the dynamics of a classical swirl injector. The dynamic response through injector components for disturbed inflow condition was investigated. The modified code was validated from comparison with the theoretical result for a typical swirl injector. Clearly the simulated result shows the interesting characteristics of swirl injectors to provide either amplification or damping of the input disturbance through each component. These results give promise in applying the current model to nonlinear dynamic characteristics of swirl injectors.

초 록

스월 인젝터의 비선형 동적특성을 모사할 수 있는 수치해석 모델을 개발하여 인젝터내의 정적/동적 특성을 분석하였다. Boundary Element Methods (BEMs)을 적용한 수치모델은 유체 경계면 산출에 매우 유리한 장점이 있어 표면의 불안정성 해석에 유용하게 적용되어 왔다. 이전의 연구 결과에서는 스월효과를 고려할 수 있도록 확장된 수치모델을 이용하여 인젝터의 형상을 고려한 정적특성을 보여주었다. 본 논문에서는 유입 흐름에 교란이 발생했을 때 인젝터의 각 구성요소에서의 동적응답을 분석하였고, 이론적 결과와 비교하여 수치모델에 대한 타당성을 검증하였다. 본 수치해석 결과는 입력류에서의 교란이 각 인젝터 구성품을 지나면서 감쇠/증폭되고 위상차를 만들게 되는 과정을 잘 모사하고 있다. 개발된 수치모델은 인젝터의 다양한 설계변수들이 유동특성에 미치는 효과 분석과 이론적 모델로는 예측이 어려운 비선형 영역에서의 동적 응답특성 분석에 유용하게 적용될 수 있을 것이다.

Key Words : Swirl Injector(스월 인젝터), Dynamic Characteristics(동특성), Film Thickness (필름 두께), Atomization(분무화), Boundary Element Method(BEM)

† 2006년 2월 8일 접수 ~ 2006년 7월 12일 심사완료
* 정회원, 국방과학연구소
연락저자, E-mail : hbpark@purdue.edu
대전시 유성구 유성우체국 사서함 35호

Ⅰ. INTRODUCTION

A swirl injector or simplex/pressure-swirl atomizer is one of the more common devices

used to atomize liquids. The hollow-cone simplex atomizer creates angular momentum by injecting the liquid tangentially into a vortex chamber. Since swirl injectors offer the advantage in the throttling and give high thrust per element, they have been intensely studied for aerospace propulsion applications over the past sixty years. In these applications, both steady-state and dynamic characteristics of the injector have been of great interest to predict bulk performance and to understand instability mechanism related to the dynamic response of engines.

One of the historical models for the classical swirl injector model as presented in Bayvel and Orzechowski [1] utilizes the principle of maximum flow to solve for liquid film conditions within the injector. This principle is borrowed from the Russian engineer Zhukovsky from his studies of water flowing over a dam; this principle directly applies to swirl injectors by simply substituting hydrostatic for centrifugal forces. The approach has been used largely by Russian scientists and engineers studying simplex atomizers [2]. As a second theory, Yule-Chinn [3] used axial momentum conservation principle to derive the equations of flow for a swirl injector without the critical assumption of the principle of maximum flow. While the utilization of the principle of maximum flow and axial momentum conservation is major difference between these two theories, predictions using the two approaches generally give similar results.

Even though many performance aspects for swirl injectors have been investigated in past studies, the nonlinear processes and the dynamic behavior of free surfaces within swirl injectors have been little studied. The motivation for the current work is to expand knowledge in these two areas. Use of Boundary Element Methods (BEMs) provides an ideal opportunity to address these issues due to the high accuracy and the ability to track free surfaces beyond atomization events. The nonlinear weak-viscous BEM model[4,5] has been effectively applied to high speed jet instability so far, but most of studies have been concentrated on the phenomenon occurred at simple cylindrical liquid jet[6,7].

On the other hand, the various static characteristics of a swirl injector for unforced inflow conditions are found in the previous study[8]. In that study, film properties such as core radius and thickness inside / outside the injector were computed for a variety of design conditions with grid convergence test. Also, the influence of injector geometry on flow characteristics was studied through parametric studies. By the way, in this study for dynamic analysis, the geometry and flow condition of the baseline injector was not changed from the previous static characteristics analysis except adding a long passage as a substitute for tangential channel. Since any discernable discrepancy for flow characteristics with/without a long channel was not found, we can refer to the previous study[8] for more detailed static characteristics of a swirl injector.

V. G. Bazarov's model[2] provides the theoretical analysis method for dynamic response of the classical injector. In this theoretical model, the tangential channel, the vortex chamber and the nozzle are analyzed independently and then combined to give the overall transfer function of the swirl injector. The analysis result provides a good comparison with our result by using BEM code. The simulated dynamic response is compared with the theoretically predicted response obtained for pressure pulsation in the feed system. In this study, on the basis of moving surface treatment method and surface instability study, which are obtained from the previous static characteristics analysis in pressure-swirl atomizers[8], this work was expanded for analyzing the dynamics of a classical swirl injector. The dynamic response through injector components for disturbed inflow condition was investigated. The calculated response showed well the dynamic behavior of a swirl injector for a forced inflow condition.

II. MODEL DESCRIPTION

2.1 BEM Method accounting for Swirl

Figure 1 provides a schematic of a classical

simplex injector noting the fluid injection via tangential channels at the head end of the vortex chamber. The gas core develops naturally as a function of the vortex chamber diameter, inlet mass flow and the degree of swirl imparted to the fluid. Key dimensions and nomenclature are noted in Fig. 1 for application to the analysis and subsequent discussion. Reference[7] provides a complete description of the basic model elements; only highlights will be presented here in the interest of brevity. An inviscid, incompressible, axisymmetric flow is presumed such that the flow dynamics are governed by Laplace's equation, $\nabla^2\phi=0$. The boundary element method utilizes an integral representation of this equation to provide a connection between ϕ values on the boundary, the local geometry, and the local velocity normal to the boundary, $q=\partial\phi/\partial n$, as follows:

$$\alpha\phi(\vec{r}_i)+\int_S\left[\phi\frac{\partial G}{\partial\hat{n}}-qG\right]ds=0 \qquad (1)$$

where $\phi(\vec{r}_i)$ is the value of the potential at a point $\vec{r}_i$, S is the boundary of the domain, α is the singular contribution when the integral path passes over the "base point", and G is the free space Green's function corresponding to Laplace's equation.

The unsteady Bernoulli equation provides a connection between the local velocity potential and the surface shape at any instant in time. For the swirling flow, modifications are required to account for the centrifugal pressure gradient created by the swirl. Without swirl, the dimensionless unsteady Bernoulli equation is as follows,

$$\frac{D\phi}{Dt}=\frac{1}{2}|\vec{u}_t|^2-\vec{u}_t\cdot\vec{u}_v-P_g-\frac{\kappa}{We}+\frac{Bo}{We}z \qquad (2)$$

where ϕ is the velocity potential and k is the local surface curvature. The Weber number ($We=\rho U^2a/\sigma$), Bond number ($Bo=\rho ga^2/\sigma$) become the dimensionless parameters governing the problem where ρ and σ are the density and the surface tension, respectively. Physically, this result is a Lagrangian form suitable for use for fluid elements moving with the local velocity of the free surface. The terms on the RHS of the equation include the effect of dynamic pressure, local gas-phase pressure, capillary, and hydrostatic pressure contributions respectively. In Eq.(2), the total surface velocity, $\vec{u}_t$, can be computed via a superposition of the base axial flow in the injector ($\phi,\vec{u}$) with a potential vortex ($\phi_v,\vec{u}_v$). Letting u,v,w represent axial, radial, and circumferential velocity components respective- ly, we may write the total velocity with a potential vortex (v) as follow:

$$\phi_t=\phi+\phi_v \quad u_t=u+u_v \quad v_t=v+v_v \quad w_t=w+w_v \qquad (3)$$

Superposition of a potential vortex can be achieved by starting with the complex potential:

$$F(z)=-\frac{i\Gamma}{2\pi}\log(z) \qquad (4)$$

where z is complex variable, Γ is vortex strength, and F is the complex potential. The resulting velocity components for this flow are as follows,

$$u_v=0, \quad v_v=0, \quad w_v=\frac{\Gamma}{2\pi r} \qquad (5)$$

and

$$\frac{1}{2}w_v^2=\frac{1}{2}\left(\frac{\Gamma}{2\pi r}\right)^2=\frac{1}{2}\left(\frac{2\pi a_0U}{2\pi r}\right)^2=\frac{1}{2}\left(\frac{a_0U}{r}\right)^2 \qquad (6)$$

Choosing the ideal injection velocity (U), the orifice radius (a), and liquid density (ρ) as dimensions, the dimensionless result can be written as,

$$\frac{D\phi}{Dt}=\frac{1}{2}|\vec{u}|^2-P_g-\frac{\kappa}{We}+\frac{Bo}{We}z-\frac{1}{2}\left(\frac{a_o}{a}\right)^2\frac{1}{r^2} \qquad (7)$$

where the Weber and Bond numbers are defined as above. Since we have nondimensionalized against the tangential velocity, U, the Rossby number does not appear explicitly in Eq.(7), but the last term on the RHS of the equation corresponds to the circumferential pressure developed by the potential vortex. In this context, the radial location of the center of the tangential channel, a_o, defines the dimensionless strength of the

vortical flow. Equation (7) are integrated in time using a 4th-order Runge-Kutta scheme to provide the evolution of the velocity potential and the motion of the free surface. Formally, the resolution of the scheme is second-order in space and 4th-order in time, but surface curvature and capillary forces are resolved with 4th-order accuracy given a set of points defining the instantaneous shape. More details regarding the numerical procedure can be found in Ref.[7].

As the surface forms a conical film when it exits the nozzle, instabilities result in the formation of annular ring-shaped ligaments. The droplet diameter after pinch-off is calculated from the linear theory due to Ponstein[10]. The growth rate, w, was related to the wave number of the disturbance, k, as follows:

$$w^2 = \left[\frac{\sigma}{\rho a_r^3}(1-k^2a_r^2)+\left(\frac{\Gamma_r}{2\pi a_r^2}\right)^2\right](ka_r)\frac{I_1(ka_r)}{I_o(ka_r)} \quad (8)$$

where a_r and Γ_r are the radius and the circulation of the vortex-ring, respectively, and I_0 and I_1 are modified Bessel functions of 0th and 1st order. When Γ_r=0, this result reduces to the classic Rayleigh result for instability of a liquid column. We have assumed that a_r is relatively smaller than the nozzle radius, a which requires $ka_r \leq 1.0$ for application validity. The equivalent circular diameter of the ring-shaped ligaments is used to determine the appropriate a_r value for each ring. Using Ponstein's result, the k value that maximizes w is determined for each ring pinched from the parent surface. Droplets are assumed to be formed instantaneously from this initial condition and the initial velocity and position of each droplet is determined assuming they are uniformly distributed about the circumference of the ring. The output from this computation is then used as the input of the droplet tracking program. Newton's 2nd law is applied to describe the motion of a droplet assuming aerodynamic drag to be the only external force acting on a droplet.

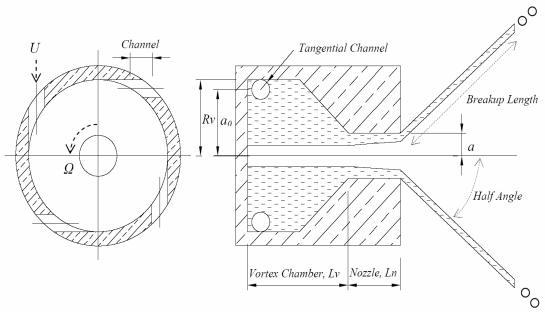

Fig. 1. A classical swirl injector noting nomenclature used for design variables

$$m_D \frac{d\vec{u}_D}{dt} = C_D \frac{1}{2}\rho_g(\vec{u}_g - \vec{u}_D)\left|\vec{u}_g - \vec{u}_D\right| A_D \quad (9)$$

where A_D is the projected area of a droplet $(\pi D^2/4)$, m_D and $\vec{u}_D$ are droplet mass and velocity, respectively. Further information regarding this approach is provided in Ref.[7].

2.2 Baseline Case Simulations

The nonlinear dynamic behavior of swirl injector is investigated by the BEM method using modified Bernoulli equation as derived in the previous section. Figure 1 provides a schematic of the injector to be analyzed. This injector was designed by the monopropellant swirl injector design procedure outlined in the Ref.[1] to size an injector for mass delivery of 9.07E-2 *kg/s* of water at a pressure drop of 0.69 *MPa*. It has a nominal spray angle of 90 *deg* and the film thickness to be approximately 0.43 *mm* at the nozzle exit. The injector geometry for this design is summarized in Table 1 below:

Table 1. Assumed Baseline Geometry for Swirl Injector Simulations

Radius to Center of Tangential Chn, a_o	= 3.226 *mm*
Radius of Nozzle, a	= 2.151 *mm*
Radius of Vortex Chamber, R_v	= 4.234 *mm*
Radius of Tangential Channel	= 0.643 *mm*
Length of Tangential Channel	= 1.516 *mm*
Length of Nozzle, L_n	= 1.500 *mm*
Length of Vortex Chamber, L_v	= 4.547 *mm*
No. of Inlet Channels	= 4
Inlet Velocity	= 17.50 *m/s*

On the other hand, the inlet shape was treated as a circular cylinder and its area was calculated according to mass flow rate. In fact, the tangential channel which is arranged circumferentially to the injector body has to be considered as a 3-dimensional problem. Since proper treatment for this tangential channel is essential to perform dynamic analysis for whole injector, the possible various methods have to be investigated. In this study, as one of the methods to treat the tangential channel in our axysimmetric code, the long channel was added simply in the inlet as a substitute for the real tangential channel. Figure 2 shows a grid system for this assumed injector geometry. In order to keep the same mass flow rate through the channel, the inlet width is linearly reduced with increasing radius. For this simulation, the non-dimensional parameters and the geometric criterion are calculated from the reference jet speed and the reference nozzle radius of $U = 17.50$ *m/sec* and $a = 2.151$ *mm*, respectively.

In addition, the corner is treated as a moving grid to form a right angle between them and the grid space along the wall is stretched according to movement of the contact point. Therefore, we do not have to know the core radius inside the injector throughout the simulation and the gas core radius appear naturally as a simulation result. For the baseline conditions described above, Reference [8] for static flow characteristic analysis with the geometric condition provided a comparison

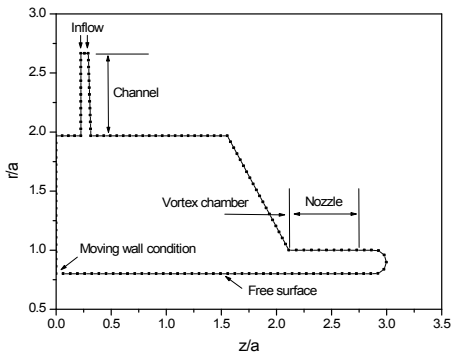

Fig. 2. Grid system having a long channel for a swirl injector

of free surface shapes in the nozzle region for various grids indicating an insensitivity to grid size for all cases investigated. Obviously, results showed no discernable difference in core radius, film thickness, velocities, and jet half angle, etc., for the meshes studied. On the other hand, as shown in Table 2, the simulation result is in reasonable agreement with the linear inviscid theory. The core radius, the film thickness and the spray angle are exactly matched with the theoretical result[1].

Table 2. Calculated result comparison against the theoretical result of V.G.Bazarov [1]

		Simulation	Theory
Core radius		0.704	0.700
Film thickness		0.205	0.200
Half angle (*deg*)		45.5	45.0
Total velocity (*m/sec*)	at nozzle entr.	19.4(at wall) 10.9(free surf.)	-
	at nozzle exit	23.5(at wall) 20.7(free surf.)	-
	outside injector	35.90	36.09
Axial velocity (*m/sec*)	through nozzle	17.45	17.37
	outside injector	26.26	26.26

III. RESULTS AND DISCUSSIONS

3.1 Analysis of Static Characteristics

The various static characteristics analyses of a swirl injector for unforced inflow conditions are found in the other paper of Ref.[8]. In this reference, film properties such as core radius and thickness inside/outside the injector were computed for a variety of design conditions. Also, the influence of injector geometry on flow characteristics was studied through parametric studies. By the way, in this study for dynamic analysis, the geometry and flow condition of the baseline injector was not changed from the previous static characteristics analysis except adding a long passage for tangential channel. Since any discernable discrepancy for flow characteristics with/without a long channel was not found, we can refer to the previous study[8] for more detailed static characteristics of a swirl injector.

In an unforced inflow condition for the baseline injector shown in Fig. 1, the radial/ axial velocity profiles with theoretical value along the fluid surface are shown in Fig. 3. Figure 4 also shows the flow structure inside the injector and this figure provides the final jet shape of a typical swirl injector with shed droplets. The reproduced jet has characteristics similar to the actual spray jet which is seen in real world. We can see clearly the core formation inside the swirl injector and the cone angle formation outside the injector in this figure. The shed droplets are moving to the same direction with the parent jet and their size distribution is almost constant. The jet shown in this figure has the flow properties of SMD/a(droplet size) = 0.185, Θ_D (cone half angle) = 45.8 deg, and U_D/U (total velocity) = 1.75. For this jet, the other statistical properties are summarized in Table 3. Figure 5 provides 3-dimensionally the whole jet evolution and the jet core structure of a classical swirl injector. The 3-dimensional movement

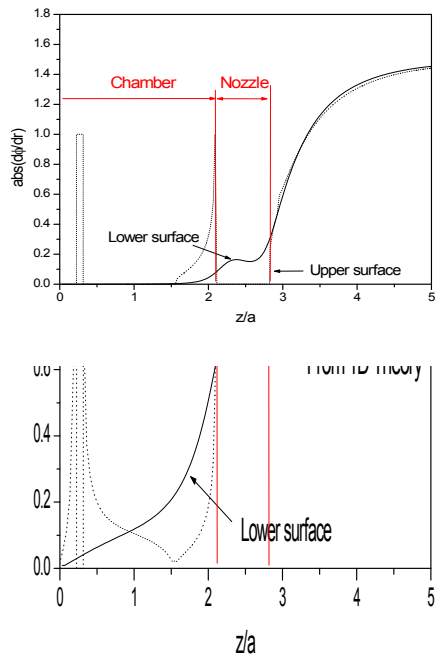

Fig. 3. Radial (up) and axial (down) velocity profile along fluid surface in aclassical swirl injector

Table 3. Statistical properties for a swirl injector

	Properties
SMD/a	0.185
N_D	1741
D_D/a	0.198
$\bar{u}_D/U$	1.21
$\bar{v}_D/U$	1.26
$\theta_D(^\circ)$	45.8

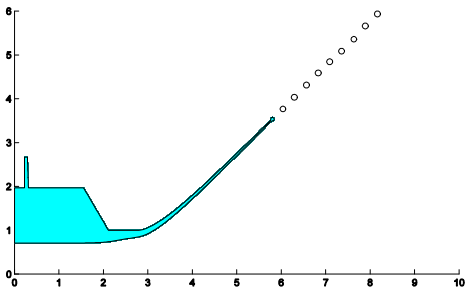

Fig. 4. Final jet shape showing shed droplets for the baseline swirl injector, at $t^*=12.0$

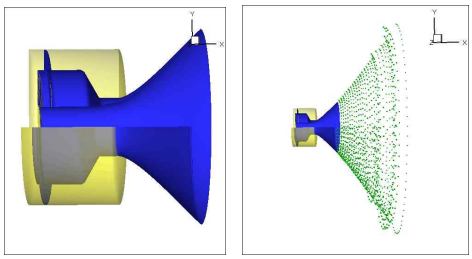

Fig. 5. 3-Dimensionally visualized final jet shape in a classical swirl injector

of shed droplets is added to the parent jet. We can see the breakup length much clearly in this figure. The breakup length is kept almost in constant after $t^*=5.0$ and shed droplets are moving downstream as the direction angle of parent jet. The overall spray is qualitatively similar to that of actual experimental image[10].

3.2 Dynamic Characteristics Analysis

Dynamic response for disturbed inflow velocity was investigated in this study. The same classical injector as shown in Fig. 1 was analyzed using our BEM model. That is, the response of the classical swirl injector having

Fig. 6. Selected locations for dynamic response analysis in a classical swirl injector

U = 17.5 m/sec for *0.69 MPa* pressure drop was studied. Figure 6 shows measured locations for dynamic response analysis in our calculation. These points were chosen for convenience for our response analysis. Since the response could be dependent on the measured location, we have to be careful to compare the result with any theoretical /experimental result.

In our simulation, since the dimensionless time in the computational domain is $t^* = U/a \cdot t$, the oscillation frequency for disturbed inflow can be set as;

$$F(\varpi^*) = A\sin(\varpi^* t^*) \tag{10}$$

where ϖ^*, A is the nondimensional wave number and the amplitude, respectively. In our study, the disturbance is set as the fluctuation of the inflow velocity in the tangential channel. In addition, the inlet for tangential channel is assumed as the circular cylinder in our axysimmetric simulation and its area is determined to have the same mass flow rate with the actual injector. In order to keep the constant area for the same mass flow rate throughout tangential channel, the channel width at the tip and the root can be calculated as;

$$W_{T,tip} = \frac{R_v}{R_v + L_T} W_{T,root}, \text{ where } W_{T,root} = \frac{4R_T^2}{2R_v} \tag{11}$$

As a first condition to investigate the dynamic response of a classical injector by using our modified BEM code, the oscillation frequency and amplitude for disturbed inflow were set as *f=5000 Hz* and *A=0.1*, respectively. This simulation takes much longer time than the cases for obtaining statistical properties because we have to confirm its repetitive behavior for several waves. Therefore, in order to save the computational cost, this simulation was restarted from the steady state solution obtained at the time of *t*=5.0*. Then, the stabilized response after about *t*=10.0* was obtained as shown in Fig. 7. Clearly, we can see the recurrent behavior for initially disturbed inflow velocity in the several waves of this figure.

The dynamic response for a single wave through a classical swirl injector is shown in Fig. 8. Each wave of this figure shows the variation in the phase and amplitude of the response at several locations for disturbed

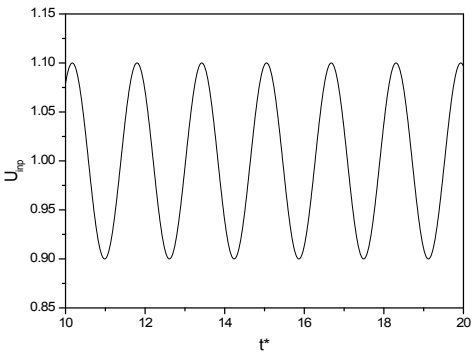

Fig. 7. Raw input (up) and response (down) for initially disturbed inflow velocity; the oscillation frequency and the amplitude were set as *f=5000 Hz* and *A=0.1*, respectively

Fig. 8. Dynamic response through a classical swirl injector, which was investigated in velocity response; the oscillation frequency and the amplitude were set as *f=5000 Hz*, *A=0.1* (up), and *f=1000 Hz*, *A=0.1* (down), respectively

inflow velocity. In the upper figure of Fig. 8, the oscillation frequency and the amplitude were set as *f=5000 Hz* and *A=0.1*, respectively. Clearly, we can see the phase shift with magnitude change due to damping and amplification through each component. The lower figure of Fig. 8 shows the dynamic response in case of relatively lower frequency. In this case, the oscillation frequency and amplitude were set as *f=1000 Hz* and *A=0.1*, respectively. From the comparison between these two frequencies, it is found that the response can be changed by the frequency range as known in the theoretical analysis of Bazarov[2].

IV. CONCLUSIONS

A fully nonlinear model accounting for swirling effect has been applied in analyzing the dynamic response for axisymmetric swirl liquid jets. The current work applied highly accurate Boundary Element Methods (BEMs) to simulate the free surface both inside the vortex chamber and within the hollow-cone/primary atomization zone outside the injector. A potential vortex was superposed to the bulk flow to simulate the swirl in assessing its static and dynamic characteristics.

On the basis of moving surface treatment method and surface instability study, which are obtained from the previous static characteristics analysis in pressure-swirl atomizers, this work was expanded for analyzing the dynamics of a classical swirl injector. The dynamic response through injector components for disturbed inflow condition was investigated. The simulated dynamic response showed a good agreement with the 1-D inviscid theoretical results. Clearly the simulated result shows the interesting characteristic of swirl injectors to provide either amplification or damping of the input disturbance through each component. Even though the current code has to be improved in treating tangential channel and in getting exact mass flow rate, the calculated response showed well the behavior of a swirl injector for a forced inflow condition. These results give promise in applying the current model to nonlinear dynamic characteristics of swirl injectors.

REFEREMCES

1) L. Bayvel and Z. Orzechowski. Liquid Atomization. *Taylor & Francis*, 1993.

2) Vladimir G. Bazarov and Vigor Yang. Liquid-Propellant Rocket Engine Injector Dynamics. *Journal of Propulsion and Power*, 14(5):797-806, Sep-Oct 1998.

3) A. J. Yule and J. J. Chinn. Swirl Atomizer Flow: Classical Inviscid Theory Revisited. *ICLASS-94,* Rouen, France, July, 1994.

4) C. A. Spangler, J. H. Hilbing, and S. D. Heister. Nonlinear modeling of jet atomization in the wind-induced regime. *Physics of Fluids*, 7:964, 1995.

5) S. S. Yoon and S. D. Heister. A fully nonlinear primary atomization. In *15th Annual Conference on Liquid Atomization and Spray Systems*, pages 36-40. ILASS, 2002. held in Madison, Wisconsin.

6) H. Park, D. Heister. A numerical strudy of primary instability on viscous high speed jets. *Computers and Fluids*, 2005, in review.

7) H. Park, S. S. Yoon and S. D. Heister. A Nonlinear Atomization Model for Computation of Drop-Size Distributions and Spray Simulations. *International Journal for Numerical Methods in Fluids*, 48:1219 -1240, 2005.

8) H. Park, and S. D. Heister, Nonlinear Simulation of Free Surfaces and Atomization in Pressure Swirl Atomizers, *Physics of Fluids*, 18:052103, 2006

9) Ponstein J. Instability of rotating cylindrical jets. *Applied Scientific Research*, 8(6):425-456, 1959.

10) D. Kim, Y. Yoon, and P. Han. Effect of flow condition and geometry on flow characteristics of a swirl injector. *ILASS 16th Conference*, Monterey, 2003.